CrossMark

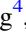# Multipoint Observation of the Solar Wind Interaction with Strong Lunar Magnetic Anomalies by ARTEMIS Spacecraft and Chang'E-4 Rover

Lianghai Xie[1,2,3] , Lei Li[1,2,3], Aibing Zhang[2], Huizi Wang[4], Quanqi Shi[4] , Jindong Wang[1,2,3], Yiteng Zhang[1,2,3], Bin Zhou[1,2,3], Yongyong Feng[1,2,3], Jinbin Cao[5], Dafei Li[6], and Shaojin Han[6]

[1] State Key Laboratory of Space Weather, National Space Science Center, Chinese Academy of Sciences, Beijing, 100190, People's Republic of China; xielianghai@nssc.ac.cn

[2] National Space Science Center, Chinese Academy of Sciences, Beijing, 100190, People's Republic of China

[3] Joint Research and Development Center of Chinese Science Academy and Shen county, Shandong, 252400, People's Republic of China

[4] Laboratory of Optical Astronomy and Solar-Terrestrial Environment, School of Space Science and Physics, Institute of Space Sciences, Shandong University, Weihai, Shandong, 264209, People's Republic of China

[5] School of Space and Environment, Beihang University, Beijing, 100191, People's Republic of China

[6] Beijing Aerospace Control Center, Beijing, 100048, People's Republic of China

Abstract

A shock or a mini-magnetosphere was once thought to be formed by the solar wind interaction with strong lunar magnetic anomalies. However, the full structure of a mini-magnetosphere has never been verified and whether a mini-magnetosphere can be completely formed remains a controversy. In this work, we present a unique multipoint observation of such an interaction by the ARTEMIS spacecraft and the Chang'E-4 rover. Both solar wind deceleration and penetration are observed by the Chang'E-4 rover on the lunar surface near the magnetic anomaly. Meanwhile, a shock is observed by the ARTEMIS spacecraft downstream from the magnetic anomaly. It is suggested that the magnetic anomaly cannot stand off the solar wind, and there is no shock but just a boundary layer near the magnetic anomaly. Accordingly, a mini-magnetosphere is not completely formed and the downstream shock observed the ARTEMIS spacecraft just corresponds to a trailing shock.

Key words: Solar wind – Lunar science – Space plasmas

1. Introduction

Differing from the Earth, the Moon has neither a global magnetic field nor a significant atmosphere. Particles from the interplanetary space, such as solar wind ions, galactic cosmic rays, and micrometeoroids, can directly bombard the lunar surface, resulting in a relatively harsher space environment. However, it has been found that the Moon possesses a large number of local crustal magnetic fields, known as magnetic anomalies (Hood et al. 2001; Mitchell et al. 2008; Tsunakawa et al. 2015), which can deflect the solar wind and form a small-scale structure with lower solar wind flux. Previously, both the Lunar Prospector (LP) and the ARTEMIS spacecraft observed shock-like structures near some strong magnetic anomalies (Lin et al. 1998; Halekas et al. 2006, 2014). Meanwhile, a reduced solar wind flux was found in the central magnetic anomaly region by the energetic neutral atom (ENA) observations of the Chandrayaan-1 spacecraft (Wieser et al. 2010; Vorburger et al. 2012), suggesting the magnetic shielding of the lunar surface from the solar wind. As a result, it seems that these strong magnetic anomalies can stand off the solar wind and form a local protecting structure, which is similar to the Earth's magnetosphere but with a smaller size, and hence it is known as a lunar mini-magnetosphere (LMM).

The question is how a magnetic field on the scale of the ion gyroradius (or ion inertial length) can form a shock. Previously, lunar magnetic anomalies were thought to be not strong enough to generate a shock but only some whistler or magnetosonic

waves, according to hybrid simulations (Omidi et al. 2002), while Hall MHD simulations showed that the nondipolar nature of lunar crustal fields could increase the lateral extent of the field and help to form a shock (Harnett & Winglee 2003; Xie et al. 2015). Additionally, there are some solar wind protons (~10%) reflected from the strong magnetic anomalies (Saito et al. 2010; Lue et al. 2011). These reflected protons can also help to slow down the solar wind and form a shock-like structure (Fatemi et al. 2014; Halekas et al. 2014). Another question is whether an LMM can completely be formed. Up to now, people have just found enhancements in the magnetic field and the plasma density near some strong magnetic anomalies, but without a density cavity. These enhancements may correspond to either the sheath of a LMM or the nose of a magnetosonic wake (Omidi et al. 2002). A density cavity was once seen by LP under some special solar wind conditions (Halekas et al. 2008), including a high solar wind density (15.8 cm^{-3}), a low solar wind velocity (303 km s^{-1}), a low solar wind temperature (1.11 eV), a high solar zenith angle (SZA; ~83°), and a low altitude (~30 km). Nevertheless, such a density cavity lied far downstream (~10° in longitude) from the magnetic anomaly, which may only represent the tail of an LMM or a magnetosonic wake. Besides, the reduced solar wind flux indicated by the ENA measurements may be just caused by a deflected solar wind velocity rather than a density cavity. Consequently, it is still uncertain whether there is a density cavity in the central magnetic anomaly region. If there is no central density cavity, the "mini-magnetosphere" may be not completely formed, and the term "mini-magnetosphere" seems inappropriate.

So far, there is no multipoint observation of the solar wind interaction with lunar magnetic anomalies, and hence the full structure of the interaction is still unknown. In addition, both
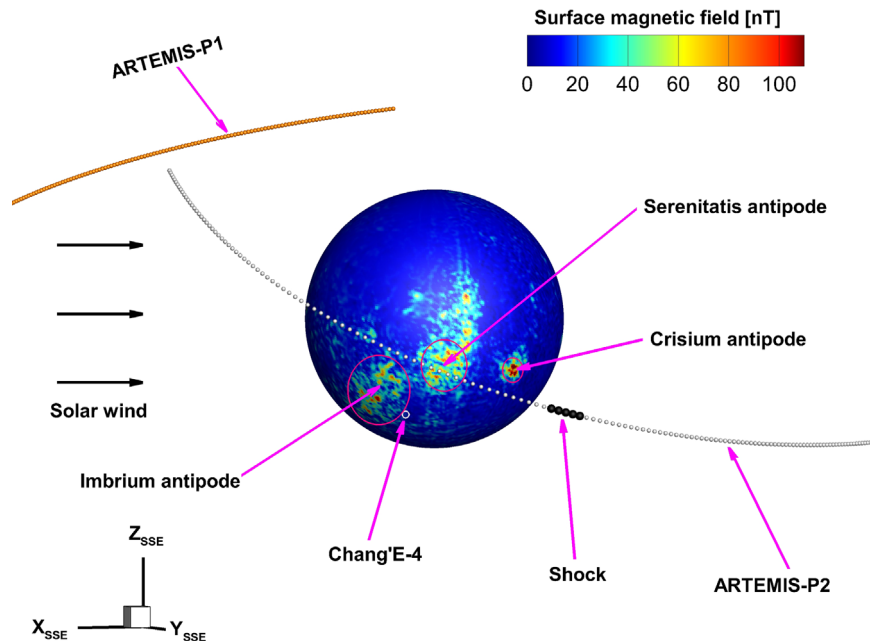
Figure 1. Observing geometries of ARTEMIS and CE-4 during 01:00-08:00 UT on 31 December 2019. The central sphere represents the lunar body with color contours to show the crustal magnetic field on the lunar surface. The white circle on the lunar surface indicates the position of CE-4. The magenta circles indicate the magnetic anomalies at the Imbrium antipode, Serenitatis antipode, and Crisium antipode, respectively. The yellow and gray dots show the trajectories of ARTEMIS P1 and P1, respectively. The solid black dots indicate the time around 02:15 UT when ARMTEMIS P2 encounters the shock. The geometries are shown in the SSE coordinate, in which the solar wind flows in the opposite direction to the X-axis and the Z-axis is normal to the ecliptic plane.

the simulations and the observations have suggested that the shock-like structure favors a smaller ion inertial length and a stronger magnetic field. Here we present a unique multipoint observation of the solar wind interaction with a group of strong lunar magnetic anomalies, in which the Chang'E-4 (CE-4) rover is located on the lunar surface near the magnetic anomalies and the ARTEMIS spacecraft are in orbit. Moreover, the multipoint observation happens under a special solar wind condition with a very small ion inertial length. As a result, this work provides a good chance to check whether a bow shock as well as a complete mini-magnetosphere can be caused by the solar wind interaction with lunar magnetic anomalies.

2. Observations

The ARTEMIS mission is the extension of the THEMIS mission, which has two identical probes, P1 and P2 (Angelopoulos [2011]). From 2011 April on, both probes operate in a high-eccentricity orbit of $\sim$100 km $\times$ 19,000 km, with an orbit period of $\sim$26 hr. When one probe is in the lunar wake, the other one is usually in the solar wind. In this way, ARTEMIS mission can measure the plasma in both the solar wind and the lunar wakes, with the fluxgate magnetometer (Auster et al. [2008]) and the electrostatic analyzer (McFadden et al. [2008]) instruments. the CE-4 mission is the first mission soft-landed on the lunar far side. The Advanced Small Analyzer for Neutrals (ASAN) onboard the rover of the CE-4 mission is an ENA analyzer, which can measure the solar wind ions that are backscattered from the lunar surface as ENAs (Wieser et al. [2020]; Zhang et al. [2020]). The incident solar wind flux on the lunar surface can be inferred with the measured ENA flux (Xie et al. [2021]). During 01:00-08:00 UT on 2019 December 31, ARTEMIS P1 was in the undisturbed solar wind upstream from the lunar wake and observed a very special solar wind, which had a high number density ($\sim$20 cm^{-3}), a low

velocity ($\sim$300 km s^{-1}), and a low temperature ($\sim$7 eV). These solar wind parameters are similar to those for the density cavity event observed by LP (Halekas et al. [2008]). Meanwhile, ARTEMIS P2 flew across the lunar wake and observed a shock around 02:15 UT before entering the wake, with an altitude of about 800 km. The shock is downstream from a group of strong magnetic anomalies (Imbrium, Serenitatis, and Crisium antipodes; see Figure [1]). During the same period of interest, the CE-4 rover was located on the lunar surface near the Imbrium antipode anomaly. An ENA spectrum was measured by ASAN of CE-4 during 05:10–06:06 UT on 2019 December 31, which was about 3 hr after the shock seen by ARTEMIS P2, but still in the period of 01:00-08:00 UT, when ARTEMIS P1 saw the special solar wind. Previously, we have found that the ion inertial length and the normal component of the solar wind dynamic pressure are two key parameters to determine the interaction between the solar wind and the lunar magnetic anomaly (Xie et al. [2021]). Here we find that these two parameters only change a little (less than 2%) between the ARTEMIS P2 and the CE-4 measurements. In addition, similar shocks were also observed by ARTEMIS P2 in the previous 2 days and the following 2 days, though the shock intensities were relatively weaker due to the different solar wind conditions, implying that a long-period shock could be caused by the solar wind interaction with these strong magnetic anomalies. As the time difference between the CE-4 and the ARTEMIS P2 measurements is about 3 hr, and the solar wind conditions for these two measurements are similar, we think that CE-4 and ARTEMIS P2 can approximately provide a two-point observation of the same interaction. The observing geometries of ARTEMIS and CE-4 during this period are shown in Figure [1], where the Selenocentric Solar Ecliptic (SSE) coordinate is used, whose X-axis points from the Moon's center to the Sun, the Z-axis is normal to the ecliptic plane, and the Y-axis completes the right-handed set of axes.
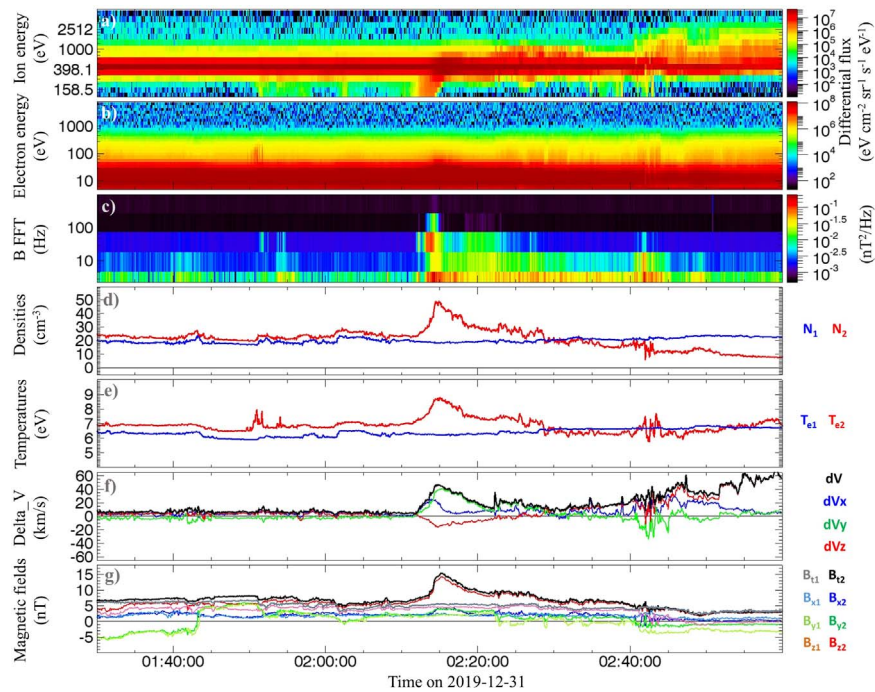
Figure 2. Shock observed by ARTEMIS. (a)–(c) show the ion energy spectrum, the electron energy spectrum, and the fast Fourier transform of magnetic field fluctuations measured by ARTEMIS P2; (d)–(g) show the number densities and the electron temperatures, the velocity differences, and the magnetic fields, respectively, in which subscripts of 1 and 2 indicate the measurements of P1 and P2, respectively, and the lines in different colors represent the different components in SSE coordinate. The black line in (f) shows the magnitude of velocity change between the upstream P1 measurements and the downstream P2 measurements. The gray and the black lines in (g) show the magnitudes of magnetic field measured by P1 and P2, respectively.

The shock observed by ARTEMIS P2 is shown in Figure 2, where we can see obvious changes in the plasma properties around 02:15 UT, including an ion deceleration (Figure 2(a)); an electron heating (Figure 2(b)), and some magnetic field fluctuations (Figure 2(c)). Furthermore, both the number density and the magnetic field are significantly enhanced by factors of 2.1 (Figure 2(d)) and 2.3 (Figure 2(g)), respectively. Meanwhile, the average electron temperature increases from 6.9 eV to 8.6 eV (Figure 2(e)), and there is also a deflection in the solar wind velocity (mainly in the Y direction), apart from the deceleration in the X direction (Figure 2(f)). The total change in the velocity is $\sim$46 km s^{-1}, which is larger than both the Alfvén velocity of $\sim$29 km s^{-1} and the magnetosonic velocity of $\sim$42 km s^{-1} of the upstream solar wind, implying a discontinuity in the flow. In addition, the magnetic field lines have been rotated across the discontinuity (Figure 2(g)). All of these features suggest a strong shock observed by ARTEMIS P2. Known from Figure 1, the shock is downstream from a group of strong magnetic anomalies, suggesting that the shock is caused by the solar wind interaction with these magnetic anomalies. Besides, it is found that the plasma properties are further changed after 02:30 UT, without returning to their undisturbed values, implying that the shock is accompanied with a long tail and may change the structure of the lunar wake.

The ASAN instrument onboard CE-4 rover can measure the backscattered ENAs in an energy range from 10 eV to 10 keV, with a typical energy resolution of 30% (Wieser et al. 2020). However, it was found that the ENA fluxes at energies lower than 100 eV could be contaminated by the sputtered ENAs from the local regolith (Zhang et al. 2020), which should be excluded when calculating the integrated ENA flux over the energy (J_{ENA}). In addition, ASAN only works in the morning and the afternoon of the local lunar day, with a typical period of

$\sim$1 hr and an SZA ranging from about 50° to 80°. In particular, ASAN is downstream from the magnetic anomaly for the afternoon measurements but upstream from the magnetic anomaly for the morning measurements. Previously, Zhang et al. (2020) found that the ENA spectra measured by ASAN showed a cutoff energy (E_{cut}) that was approximately equal to the solar wind energy (E_{sw}), at which the ENA flux can drop to the instrument sensitivity level. Additionally, Xie et al. (2021) found that the J_{ENA} measured by CE-4 could almost linearly increase with the normal component of the solar wind flux on the lunar surface ($J_{sw,N}$), but the J_{ENA} measured downstream from the magnetic anomaly were generally lower, suggesting a magnetic shielding caused by the magnetic anomaly. Wang et al. (2021) found that that the E_{cut} downstream from the magnetic anomaly was lower than those upstream from the magnetic anomaly, implying solar wind deceleration by the magnetic obstacle.

Here we choose three ENA spectra measured during the periods of 05:10–06:06 UT on 2019 December 31, 09:43–10:37 UT on 2020 October 12, and 07:11–08:12 UT on 2020 September 13, respectively, and call them Case 1, Case 2, and Case 3, respectively. Case 1 is downstream from the magnetic anomaly, which happens during the same period of the ARTEMIS observation. Case 2 and Case 3 are upstream from the magnetic anomaly, which are used to compare with Case 1 to show the effect of magnetic anomalies on the solar wind. As shown in Figure 3, in Case 2 and Case 3, the E_{cut} is almost equal to the E_{sw} and the J_{ENA} almost linearly increases with the $J_{sw,N}$, which is consistent with the previous conclusions obtained by Zhang et al. (2020) and Xie et al. (2021). Case 1 and Case 3 have similar E_{sw}, and we may expect similar E_{cut} in these two cases. However, it is found that the ENAs in Case 1 are more gathered at lower energies with a
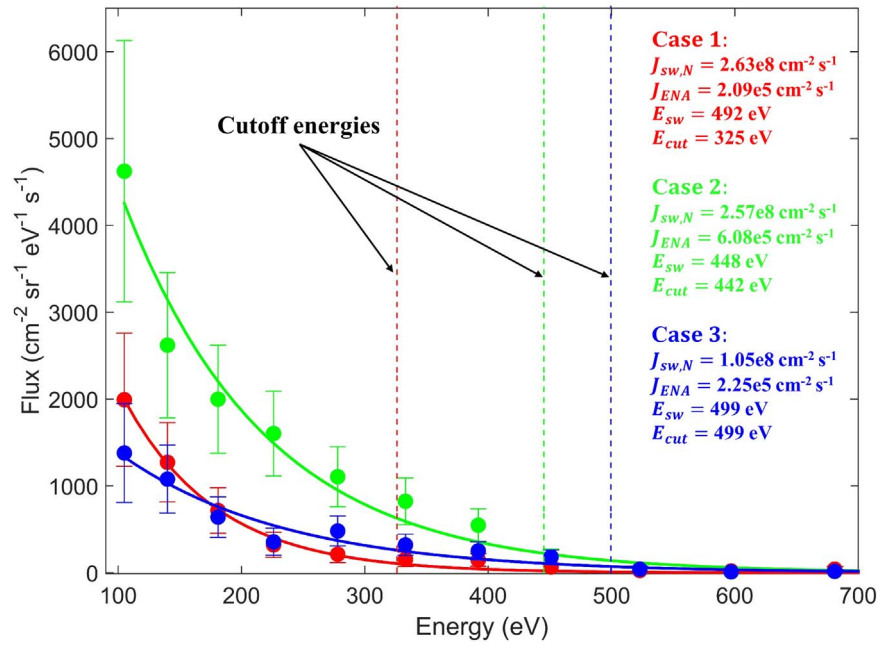
Figure 3. ENA spectra observed by CE-4. The red, green, and blue dots show the measured spectra of Case 1, Case 2, and Case 3, respectively, in which Case 1 is downstream from the magnetic anomaly and correlated with the LMM observed by ARTEMIS, while Case 2 and Case 3 are upstream from the magnetic anomaly with similar solar wind conditions to those of Case 1. The solid lines are the fitting results of the three spectra with exponential functions. The dashed lines indicate the cutoff energies, at which the ENA flux is equal to 5.4% of its initial flux at 105 eV. Texts on the right show the parameters of the three cases, in which $J_{sw,N}$ is the normal component of the solar wind flux on the lunar surface; J_{ENA} is the integrated ENA flux over the energy; E_{sw} is the solar wind energy; and E_{cut} is the cutoff energy.
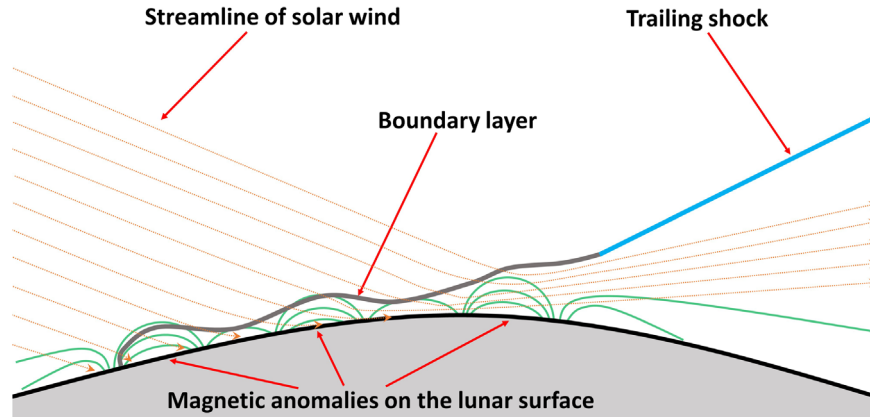

Figure 4. Schematic diagram of the solar wind interaction with lunar magnetic anomalies. The green lines indicate the magnetic anomalies on the lunar surface. The dotted red lines indicate the streamlines of the solar wind. The solid gray line indicates the boundary layer near the magnetic anomalies. The solid cyan line shows the trailing shock downstream from the magnetic anomalies.

smaller E_{cut} (see the red and blue lines in Figure 3), suggesting that the solar wind ions have been decelerated by the magnetic anomaly. Case 1 and Case 2 have similar $J_{sw,N}$, and the J_{ENA} in these two cases may be very close, as we have found that the J_{ENA} almost linearly depends on $J_{sw,N}$ (Xie et al. 2021). Nevertheless, here the J_{ENA} for Case 1 is only about $1/3$ that of Case 2, which suggests that the solar wind has been partially shielded by the magnetic anomaly. However, it also implies that part of the solar wind ions have penetrated into the magnetic obstacle. As a result, the lunar surface is not fully shielded from the solar wind and there should be no complete LMM.

3. Discussions and Implications

Based on the multipoint observations shown above, we obtain a new physical picture for the solar wind interaction with lunar magnetic anomalies. As shown in the Figure 4, a lunar magnetic anomaly has many substructures, and the interaction between the solar wind and the magnetic anomaly can be regarded as the sum of the solar wind interactions with all of these substructures. For an individual substructure, the magnetic field is not strong enough to stop the solar wind, but only deflect the solar wind. The deflection is not obvious near the nose of the interaction region and a large number of solar wind particles can penetrate across the magnetic field and impact the lunar surface. Accordingly, there is no shock but only a magnetosonic wake in this region, where the solar wind can be slightly decelerated and compressed. When moving

downstream, the solar wind can be further deflected by the following substructures, and the magnetosonic wake is getting more and more significant. Moreover, the magnetosonic wakes caused by different substructures may overlap each other, which jointly form a boundary layer near the lunar surface. Besides, some solar wind ions can be reflected by the magnetic anomaly, which can help decelerate and compress the incoming solar wind. Finally, the solar wind can flow horizontally or even outwardly from the local surface, and a trailing shock appears downstream from the magnetic anomaly. It suggests that a bow shock as well as a complete mini-magnetosphere are not formed here, even if the interaction is expected to be in an obvious fluid manner.

Our results imply that a lunar mini-magnetosphere may be never completely formed. As a result, the term of "mini-magnetosphere" should be not appropriate, which needs to be carefully used or redefined. In addition, if the lunar surface is not fully shielded by the magnetic anomaly, all applications associated with the magnetic shielding, such as the formation of a lunar swirl and the protection of a lunar station, need to be reassessed. It should be noted that a small-scale density cavity (<10 km) may exist in the central magnetic anomaly region with a very strong magnetic field ($\sim$500 nT), according to the particle-in-cell simulations done by Deca et al. (2014, 2015). Such a small-scale density cavity is very hard to be observed but may be important for the formation of lunar swirls, which needs to be further investigated in the future.

ORCID iDs

Lianghai Xie ⬤ https://orcid.org/0000-0001-9635-4644
Quanqi Shi ⬤ https://orcid.org/0000-0001-6835-4751

References

Angelopoulos, V. 2011, SSRv, 165, 3
Auster, H. U., Glassmeier, K. H., Magnes, W., et al. 2008, SSRv, 141, 235
Deca, J., Divin, A., Lapenta, G., et al. 2014, PhRvL, 112, 151102
Deca, J., Divin, A., Lembège, B., et al. 2015, JGRA, 120, 6443
Fatemi, S., Holmstrom, M., Futaana, Y., et al. 2014, JGRA, 119, 6095
Halekas, J. S., Brain, D. A., Mitchell, D. L., Lin, R. P., & Harrison, L. 2006, GeoRL, 33, L08106
Halekas, J. S., Delory, G. T. D., Brain, A., Lin, R. P., & Mitchell, D. L. 2008, P&SS, 56, 941
Halekas, J. S., Poppe, A. R., McFadden, J. P., et al. 2014, GeoRL, 41, 7436
Harnett, E. M., & Winglee, R. 2003, JGRA, 108, 1088
Hood, L. L., Zakharian, A., Halekas, J., et al. 2001, JGR, 106, 27825
Lin, R. P., Mitchell, D. L., Curtis, D. W., et al. 1998, Sci, 281, 1480
Lue, C., Futaana, Y., Barabash, S., et al. 2011, GeoRL, 38, L03202
McFadden, J. P., Carlson, C. W., Larson, D., et al. 2008, SSRv, 141, 277
Mitchell, D. L., Halekas, J. S., Lin, R. P., et al. 2008, Icar, 194, 401
Omidi, N., Blanco-Cano, X., Russell, C. T., Karimabadi, H., & Acuna, M. 2002, JGRA, 107, 1487
Saito, Y., Yokota, S., Asamura, K., et al. 2010, SSRv, 64, 4
Tsunakawa, H., Takahashi, F., Shimizu, H., Shibuya, H., & Matsushima, M. 2015, JGRE, 120, 1160
Vorburger, A., Wurz, P., Barabash, S., et al. 2012, JGRA, 117, A07208
Wang, H. Z., Xiao, C., Shi, Q. Q., et al. 2021, ApJL, 922, L41
Wieser, M., Barabash, S., Futaana, Y., et al. 2010, GeoRL, 37, L05103
Wieser, M., Barabash, S., Wang, X. D., et al. 2020, SSRv, 216, 73
Xie, L., Li, L., Zhang, A., et al. 2021, GeoRL, 48, e2021GL093943
Xie, L., Li, L., Zhang, Y., et al. 2015, JGRA, 120, 6559
Zhang, A., Wieser, M., Wang, C., et al. 2020, P&SS, 189, 104970